Research Square

Preprints are preliminary reports that have not undergone peer review.
They should not be considered conclusive, used to inform clinical practice,
or referenced by the media as validated information.

Dissecting genomic regions and candidate genes for root traits at the seedling stage under cold stress in rice

Gurjeet Singh
Texas A&M AgriLife Research and Extension Center
Sejuti Mondal
Texas State University
Rubab Iqbal
University of Agriculture
Rubeena Yasmin Shaik
Texas State University
Subroto Das Jyoti
Texas A&M University
Sanjoy K. Debsharma
Texas A&M AgriLife Research and Extension Center
Ishwarya Lakshmi VG
Texas A&M AgriLife Research and Extension Center
Chersty L. Harper
Texas A&M AgriLife Research and Extension Center
Shyamal K. Talukder
shyamal.talukder@ag.tamu.edu

Texas A&M AgriLife Research and Extension Center

Article

Keywords: Cold stress, Root, GWAS, Rice, Cold tolerance

Posted Date: June 22nd, 2026

DOI: https://doi.org/10.21203/rs.3.rs-9904314/v1

License: This work is licensed under a Creative Commons Attribution 4.0 International License. Read Full License

Additional Declarations: No competing interests reported.

Version of Record: A version of this preprint was published at Scientific Reports on October 22nd, 2026. See the published version at https://doi.org/10.1038/s41598-026-72771-w.

Abstract

Root system architecture (RSA) is crucial for plant growth under abiotic stress including cold stress (CS) in rice and capturing RSA variation under CS is a key strategy for improving cold tolerance (CT). This study aims to identify the genomic regions associated with RSA traits under CS in 204 diverse rice germplasms. Two growth environments were used: growth chamber (E1; 10°C in 1–2 weeks, followed by 17°C during weeks 3–4) and controlled greenhouse (E2; 28–30°C night/day). A total of 2448 roots were harvested four weeks after planting, and four plant biomasses, along with eight RSA traits, were measured using WinRhizo Pro. Significant phenotypic variations were observed for study traits. 8,54,832 polymorphic SNPs were used for GWAS using the FarmCPU model within the 'rMVP' package and 143 QTNs were identified (87 in E1 and 56 in E2) associated with the studied traits. Among the identified QTNs, 49 novel QTNs were multi-trait (≥ two traits), which were further used for candidate genes identification, resulting in 74 putative genes within ± 100 kb genomic regions. Key candidate genes (*OsBRD1/OsDWARF*, *MHZ11*, and *OsSNDP1*) supporting the rice root adaptation under CS by coordinated brassinosteroid biosynthesis, ethylene signaling, and phospholipid-mediated root hair development, whereas *OsPP2C27*, *OsNIP1;2*, *OsNAR2.1*, *OsMYB305*, *OsSWEET3a*, and *OsHMA7* genes play important roles in stress signaling, nutrient uptake, growth regulation, and root development. Overall, this study provides the foundation of novel insights for improving rice CT by RSA.

Introduction

Rice (*Oryza sativa* L.) is a staple food for more than half of the world's population and is one of the most important and economical sources of calories among the cereal crops [1, 2]. Climate change is increasingly threatening global food production, while plant breeding remains essential for feeding a growing population [3]. Under changing climatic conditions, belowground traits such as root system architecture (RSA) play a key role in minimizing stress impacts and sustaining plant growth and development [4]. Rice roots are integral to metabolite synthesis and strongly influence above-ground agronomic traits, contributing to efficient resource uptake and resilience under abiotic stresses like cold [5, 6]. Rice with a robust root system exhibits enhanced stress tolerance and stronger competitive ability against weeds in direct-seeded cultivation [7, 8].

Cold stress (CS), including injuries from chilling and freezing is one of the most significant abiotic stresses for agricultural crop production [9]. As rice originated from the tropical and subtropical areas, it requires a fairly high temperature, therefore, it's highly sensitive to low-temperature (LT) stress [10]. CS can severely impair rice at multiple developmental stages, from reduced germination and seedling growth to suppressed tillering and increased plant mortality. It also delays flowering and disrupts reproductive development and maturity, ultimately causing significant yield losses [11, 12]. For instance, at the booting stage, LT impact on panicle branching and pollen fertility ultimately reduces the number of grains per panicle and lowers the seed-setting rate [13]. Both the vegetative and reproductive stages of cereal development are affected by CS, which causes morphological, physiological, and cellular responses [14].

CS profoundly affects rice roots at the seedling stage, damaging root tissues and substantially reducing root growth, water absorption, and nutrient uptake [5]. This damage is linked to oxidative stress in the roots, characterized by the accumulation of reactive oxygen species (ROS) such as hydrogen peroxide, increased malondialdehyde contents, and electrolyte leakage, which indicate cell membrane damage [6]. Rice cultivars with better cold tolerance (CT) tend to have lower hydrogen peroxide levels in roots but higher levels in shoots, implying this root oxidative stress is a key factor in cold sensitivity [15]. Understanding RSA variation under CS is especially relevant as the root system is the first organ exposed to soil-based temperature changes. These physiological changes are governed by underlying

genetic mechanisms that can be harnessed in breeding programs. Therefore, there is a critical need to identify cold-responsive genes associated with root development and architecture using genomic based approaches.

Recent research has identified several key genes and regulatory pathways that can be targeted to improve rice resilience to LT at different growth stages. The *OsNCED5* gene, a chloroplast-localized enzyme involved in abscisic acid (ABA) biosynthesis, is induced by CS and plays a crucial role in maintaining ROS homeostasis which enhance the CT [16]. *OsABF1*, and *bZIP* TFs (transcription factors) in the ABA signaling pathway, are also influenced by CS, reinforcing ABA-mediated gene regulation in CT [17]. CBF/DREB family in rice leads to enhanced CT without growth penalties these TFs regulate downstream cold-responsive genes [18]. Genetic mapping and functional investigations have identified *qLTG3*, *LTG1*, *COLD1*, *CTB4a*, *bZIP73*, and *HAN1* as key factors to rice's ability to withstand cold at different developmental stages [19, 20].

The next-generation sequencing technology coupled with the upward number of genome sequences opens the opportunity to redesign genotyping strategies for more effective genetic mapping and genome analysis. In recent years, GWAS (genome-wide association study) has been widely used as a powerful tool to dissect the complex traits in rice [21–23]. In this decades, several GWAS have been conducted in rice at the germination and seedling stages under LT conditions [19, 22, 24–27]. CS strongly affects root traits, yet few GWAS have targeted root traits under CS. In a study, 185 winter faba bean genotypes were evaluated, and nine novel QTLs associated with root-related traits were identified under extreme cold conditions [28]. GWAS have identified numerous QTLs controlling rice RSA at the normal seedling stage, providing a foundation for CS studies. These include 78 RSA-related QTLs from 167 *japonica* accessions [29], 112 root-related QTLs identified in a core collection of 180 Vietnamese varieties [30], 24 QTLs governing rooting ability from 145 accessions [31], 13 root-trait QTLs detected in 391 accessions from the 3K RGP (Rice Genome Project) [32], the major root-length QTL *qRLR10* linked to F-box genes from 220 accessions [33], and 11 significant SNPs for root length and root dry weight identified in 188 accessions [34]. Despite these advances, most QTLs were identified under normal growing conditions, highlighting further need for GWAS to target root traits under CS in rice. Till date, to our best knowledge, no GWAS has investigated RSA under CS in rice, representing a critical gap in our understanding of stress-adaptive root traits. In this study, diverse rice germplasm was screened under CS and controlled conditions, followed by GWAS and candidate gene mining to identify genetic loci associated with RSA traits.

Results

Phenotypic variability

Visual comparisons demonstrated that roots of the same genotype differed significantly in overall architecture across temperature conditions, including changes in root length and root density (Fig. 1). Significant differences were observed among all genotypes and both environments for traits studied, indicating significant genetic variation was observed (Table 1). Across the two environments, significant phenotypic variation was observed for all RSA and biomass traits (Table 1). TRL averaged 15.42 ± 7.99 (range 2.54–50.18) in E1 and 606.90 ± 142.91 (range 319.90-1050.49) in E2, with a pooled mean of 311.16 ± 72.09 (range 166.43-527.02). RPA also showed wide variation, with means of 0.46 ± 0.19 (range 0.12–1.55) in E1 and 15.73 ± 4.34 (range 8.22–31.70) in E2, while the pooled dataset averaged 8.09 ± 2.23 (range 4.23–15.91). Likewise, TRSA ranged from 0.39–4.89 in E1 (1.45 ± 0.62) and 25.84–99.60 in E2 (49.42 ± 13.92), with pooled values of 25.48 ± 7.02 (range 13.29-50.00). Biomass traits were also highly variable; for example, FSW averaged 0.06 ± 0.04 (range 0.001–0.05) in E1 and 0.73 ± 0.23 (range 0.31–1.55) in E2, with a pooled mean of 0.39 ± 0.12 (range 0.19–0.81).

Table 1
Details of statistics analysis for root system architecture traits evaluated under cold and controlled condition in rice

Trait	Factor	DF	MSS#	Mean ± SD	Range	CV (%)	h^2
TRL	E1	203	127.990**	15.42 ± 7.99	2.54–50.18	48.36	0.63
	E2		209022.000*	606.90 ± 142.91	319.90-1050.49	30.87	0.19
	Pool		20187	311.16 ± 72.09	166.43-527.02	118.22	0.88
RPA	E1	203	0.079***	0.46 ± 0.19	0.12–1.55	38.11	0.43
	E2		39.32	15.73 ± 4.34	8.22–31.70	35.99	0.23
	Pool		19	8.09 ± 2.23	4.23–15.91	120.75	0.52
TRSA	E1	203	0.789***	1.45 ± 0.62	0.39–4.89	38.11	0.43
	E2		388.1	49.42 ± 13.92	25.84–99.60	35.99	0.26
	Pool		192	25.48 ± 7.02	13.29-50.00	120.75	0.48
ARD	E1	203	0.011***	0.34 ± 0.07	0.20–0.67	20.58	0.33
	E2		0.001	0.25 ± 0.02	0.19–0.31	12.21	0.40
	Pool		0.006***	0.30 ± 0.03	0.21–0.46	28.03	0.20
RV	E1	203	0.0000348***	0.01 ± 0.004	0.003–0.03	32.25	0.17
	E2		0.027	0.32 ± 0.11	0.14–0.77	46.38	0.71
	Pool		0.014	0.16 ± 0.05	0.07–0.78	126.87	0.34
RT	E1	203	3779.000***	66.28 ± 43.47	3.00-324.50	63.48	0.38
	E2		1297089	3713.68 ± 805.32	1962.00-6179.75	30.31	0.21
	Pool		644500	1889.89 ± 405.08	992.25-3202.12	119.22	0.60
RF	E1	203	8208.000***	87.96 ± 64.06	0.00-482.00	65.10	0.28
	E2		11031919	8013.61 ± 2348.60	3565.75-15397.25	39.67	0.17
	Pool		5460000	4050.79 ± 1180.92	1832.87-7804.62	126.39	0.33
RC	E1	203	398.800***	16.81 ± 14.12	0.00–86.00	83.02	0.18
	E2		1169360	2359.67 ± 764.64	1023.75-5207.25	44.800	0.50

DF=degree of freedom; MSS#=mean sum of squares from ANOVA, here E1 and E2 MSS values correspond to the genotype effect, whereas the pooled MSS represents the genotype × environment (G×E) interaction effect; SD=standard deviation; CV= coefficient of variation; h^2=broad-sense heritability; E1 = growth chamber cold condition, and E2 = controlled greenhouse condition. TRL=total root length; RPA=root projected area; TRSA=total root surface area; ARD =average root diameter; RV=root volume; RT= root tips; RF=root forks; RC=root crossings (RC); FSW=fresh shoot weight; DSW dry shoot weight; FRW=fresh root weight; and DRW = dry root weight. ***, **, *Significant at $p < 0.001$, 0.01 and 0.05, respectively.

Trait	Factor	DF	MSS#	Mean ± SD	Range	CV (%)	h^2
	Pool		581000	1188.24 ± 383.93	512.25-2611.25	130.36	0.21
FSW	E1	203	0.0032812*	0.06 ± 0.04	0.001–0.04	77.06	0.26
	E2		0.114***	0.73 ± 0.23	0.31–1.55	38.39	0.38
	Pool		0.06*	0.39 ± 0.12	0.19–0.81	111.69	0.72
DSW	E1	203	0.00004622	0.008 ± 0.004	0.001–0.06	70.84	0.55
	E2		0.00921***	0.20 ± 0.06	0.08–0.52	39.62	0.30
	Pool		0.005	0.10 ± 0.03	0.04–0.26	121.97	0.40
FRW	E1	203	0.0007211***	0.04 ± 0.01	0.003–0.09	34.34	0.49
	E2		0.1811**	0.68 ± 0.30	0.19–1.74	50.39	0.59
	Pool		0.09*	0.36 ± 0.15	0.10–0.91	126.02	0.46
DRW	E1	203	0.000012201***	0.006 ± 0.002	0.001–0.01	40.58	0.36
	E2		0.002453**	0.11 ± 0.03	0.05–0.24	37.02	0.43
	Pool		0.0012	0.05 ± 0.01	0.02–0.12	117.07	0.32

DF=degree of freedom; MSS#=mean sum of squares from ANOVA, here E1 and E2 MSS values correspond to the genotype effect, whereas the pooled MSS represents the genotype × environment (G×E) interaction effect; SD=standard deviation; CV= coefficient of variation; h^2=broad-sense heritability; E1 = growth chamber cold condition, and E2 = controlled greenhouse condition. TRL=total root length; RPA=root projected area; TRSA=total root surface area; ARD =average root diameter; RV=root volume; RT= root tips; RF=root forks; RC=root crossings (RC); FSW=fresh shoot weight; DSW dry shoot weight; FRW=fresh root weight; and DRW = dry root weight. ***, **, *Significant at $p < 0.001$, 0.01 and 0.05, respectively.

Broad-sense heritability estimates varied across traits and environments, reflecting the influence of both genetic and environmental factors. In E1, heritability ranged from 0.17 for RV to 0.63 for TRL, while in E2, it ranged from 0.17 for RF to 0.71 for RV in pool analysis h^2 ranged from 0.20 ARD to 0.88 TRL (Table 1). The distribution of all measured root traits across genotypes demonstrated a normal and continuous frequency in both environmental conditions (Fig. 2), indicating all traits as quantitative and polygenic inheritance. The coefficient of variation (CV) revealed moderate to high phenotypic dispersion across traits, with CV values ranging from 12.21% (ARD in E2) to 83.02% (RC in E1). Under individual environments, root biomass and count-related traits (RT, RF, RC) showed comparatively higher CVs, indicating larger variability among genotypes. In the pooled dataset, CVs were generally much higher from 28.03% (ARD) to 130.36% (RC), reflecting increased variation when data were combined across conditions. Pearson's correlation analysis revealed strong and highly significant positive correlations among most of RSA traits in both environments (Fig. 3). TRL observed highest correlation (r = > 0.9) with RPA, TRSA, RT, RC, and RV in E1, E2, and combined analysis of both environments. ARD showed negative correlation in E1 while positive association in E2 in the study traits. DRW showed positive association (r = > 0.7) TRL, RPA, TRSA, RV, RF, FSW, DSW, and REW in E2 and combined analysis while TRL, RPA, TRSA, and RV in E1.

Genome-wide association studies (GWAS), multi-trait and co-localize QTNs

BLUE values were used to detect QTNs within each environment, and GWAS was conducted using the FarmCPU method implemented in the rMVP package in R. A total of 143 significant QTNs were identified, which were distributed across all chromosomes (Table S1). For all the twelve traits in both years, significant QTNs were considered with LOD scores of ≥ 4.0, shown in Manhattan and quantile-quantile (Q-Q) plots (Fig. S1-S6). Among the identified QTNs, 87 and 56 QTNs were identified in E1 and E2, respectively. Across the environments, QTNs were most abundant on chromosome 3 (n = 26), followed by chromosomes 7 and 10 contributing 24 QTNs each, whereas only three QTNs were detected on chromosome 8. A total of 49 QTNs (as genetic loci) were identified as multi-trait with more than two traits (Table 2). Among these, 16, 21, 7, 1, 3, and 1 genetic loci were associated with two, three, four, five, six, and eight traits, respectively. Four multi-trait loci were identified in E2, whereas 45 were detected in E1. Chromosomes 3 and 7 harbored the highest number of multi-trait loci (n = 10 each), whereas chromosome 1 contained the fewest (n = 2). S07_25857798 genetic loci located on chromosome 7 was associated with eight QTNs namely, *qDRW_CS_7.1*, *qDRW_CS_7.6*, *qFRW_CS_7.2*, *qFSW_CS_7*, *qRF_CS_7.2*, *qRPA_CS_7.8*, *qRV_CS_7.1*, and *qTRL_CS_7.3* under E1. Six traits were associated with these genetic loci viz., S04_33155690 (*qRC_CS_4.1*, *qRF_CS_4.2*, *qRPA_CS_4.5*, *qRV_CS_4.8*, *qTRL_CS_4.3*, and *qTRSA_CS_4.5*), S07_25857799 (*qDRW_CS_7.2*, *qRF_CS_7.3*, *qRPA_CS_7.9*, *qRV_CS_7.2*, *qTRL_CS_7.4*, and *qTRSA_CS_7.7*), and S07_25857831 (*qDRW_CS_7.3*, *qRF_CS_7.4*, *qRPA_CS_7.10*, *qRV_CS_7.3*, *qTRL_CS_7.5*, and *qTRSA_CS_7.8*) identified in E1. Among the 143 QTNs identified, 25 overlapped/co-localized with previously reported QTLs/QTNs for RSA traits detected under normal growth, salt, and drought conditions in rice (Table S1). Of these, 14 were detected under CS conditions (E1) and 11 under the control environment (E2), while no prior GWAS has reported RSA-associated loci specifically under CS.

Table 2
Detailed information of multi-trait loci associated root system architecture traits under cold and controlled condition in rice

S. No.	Marker ID	Marker position (bp)	chr.	QTN name	Trait name	Environment	Env name	P value	LOD score
1	S01_5704110	5704110	1	*qDRW_CS_1*	DRW	E1	CS	2.62E-05	4.58
				qRPA_CS_1	RPA	E1	CS	8.48E-05	4.07
				qRV_CS_1	RV	E1	CS	4.49E-05	4.35
				qTRSA_CS_1	TRSA	E1	CS	8.52E-05	4.07
2	S01_25632084	25632084	1	*qRPA_C_1*	RPA	E2	C	6.72E-05	4.17
				qTRL_C_1.1	TRL	E2	C	7.74E-05	4.11
3	S02_20226093	20226093	2	*qRPA_C_2*	RPA	E2	C	8.54E-05	4.07
				qTRL_C_2	TRL	E2	C	9.42E-05	4.03
4	S02_23143820	23143820	2	*qRPA_CS_2.1*	RPA	E1	CS	6.69E-05	4.17
				qRV_CS_2.1	RV	E1	CS	8.35E-06	5.08
				qTRSA_CS_2.1	TRSA	E1	CS	6.69E-05	4.17
5	S02_34081980	34081980	2	*qRPA_CS_2.2*	RPA	E1	CS	7.45E-05	4.13
				qRV_CS_2.2	RV	E1	CS	7.39E-05	4.13
				qTRSA_CS_2.2	TRSA	E1	CS	7.47E-05	4.13
6	S03_22409823	22409823	3	*qRV_CS_3.1*	RV	E1	CS	7.33E-05	4.13
				qTRL_CS_3.2	TRL	E1	CS	2.69E-05	4.57
7	S03_22599359	22599359	3	*qRV_CS_3.4*	RV	E1	CS	7.33E-05	4.13

TRL=total root length, RPA=root projected area, TRSA=total root surface area, ARD =average root diameter, RV=root volume, RT= root tips, RF=root forks, RC=root crossings (RC), FSW=fresh shoot weight, DSW dry shoot weight, FRW=fresh root weight, and DRW = dry root weight. E1 = growth chamber cold stress (CS) condition and E2 = controlled (C) greenhouse condition.

S. No.	Marker ID	Marker position (bp)	chr.	QTN name	Trait name	Environment	Env name	P value	LOD score
				qTRL_CS_3.3	TRL	E1	CS	2.69E-05	4.57
8	S03_22720027	22720027	3	*qRPA_CS_3.1*	RPA	E1	CS	6.14E-05	4.21
				qRV_CS_3.5	RV	E1	CS	6.85E-05	4.16
				qTRSA_CS_3.1	TRSA	E1	CS	6.14E-05	4.21
9	S03_22720106	22720106	3	*qRPA_CS_3.2*	RPA	E1	CS	6.14E-05	4.21
				qRV_CS_3.6	RV	E1	CS	6.85E-05	4.16
				qTRSA_CS_3.2	TRSA	E1	CS	6.14E-05	4.21
10	S03_22720369	22720369	3	*qRPA_CS_3.3*	RPA	E1	CS	6.14E-05	4.21
				qRV_CS_3.7	RV	E1	CS	6.85E-05	4.16
				qTRSA_CS_3.3	TRSA	E1	CS	6.14E-05	4.21
11	S03_22770232	22770232	3	*qRV_CS_3.8*	RV	E1	CS	1.00E-04	4.00
				qTRL_CS_3.4	TRL	E1	CS	3.30E-05	4.48
12	S03_22855374	22855374	3	*qRPA_CS_3.4*	RPA	E1	CS	1.55E-05	4.81
				qRV_CS_3.9	RV	E1	CS	2.62E-05	4.58
				qTRL_CS_3.5	TRL	E1	CS	3.23E-05	4.49
				qTRSA_CS_3.4	TRSA	E1	CS	1.54E-05	4.81
13	S03_22890371	22890371	3	*qRPA_CS_3.5*	RPA	E1	CS	9.24E-05	4.03
				qRV_CS_3.10	RV	E1	CS	5.28E-05	4.28
				qTRSA_CS_3.5	TRSA	E1	CS	9.23E-05	4.03

TRL=total root length, RPA=root projected area, TRSA=total root surface area, ARD =average root diameter, RV=root volume, RT= root tips, RF=root forks, RC=root crossings (RC), FSW=fresh shoot weight, DSW dry shoot weight, FRW=fresh root weight, and DRW = dry root weight. E1 = growth chamber cold stress (CS) condition and E2 = controlled (C) greenhouse condition.

S. No.	Marker ID	Marker position (bp)	chr.	QTN name	Trait name	Environment	Env name	P value	LOD score
14	S03_22960436	22960436	3	*qRPA_CS_3.6*	RPA	E1	CS	2.74E-05	4.56
				qRV_CS_3.11	RV	E1	CS	5.96E-05	4.22
				qTRL_CS_3.7	TRL	E1	CS	3.02E-05	4.52
				qTRSA_CS_3.6	TRSA	E1	CS	2.73E-05	4.56
15	S03_33909336	33909336	3	*qRPA_CS_3.7*	RPA	E1	CS	5.20E-06	5.28
				qRV_CS_3.12	RV	E1	CS	8.95E-07	6.05
				qTRSA_CS_3.7	TRSA	E1	CS	5.21E-06	5.28
16	S04_14337908	14337908	4	*qRPA_CS_4.1*	RPA	E1	CS	1.88E-05	4.73
				qRV_CS_4.1	RV	E1	CS	1.36E-05	4.87
				qTRSA_CS_4.1	TRSA	E1	CS	1.89E-05	4.72
17	S04_14354356	14354356	4	*qDRW_CS_4.1*	DRW	E1	CS	1.37E-05	4.86
				qRPA_CS_4.2	RPA	E1	CS	1.75E-05	4.76
				qRV_CS_4.3	RV	E1	CS	1.07E-05	4.97
				qTRSA_CS_4.2	TRSA	E1	CS	1.76E-05	4.75
18	S04_14380680	14380680	4	*qDRW_CS_4.2*	DRW	E1	CS	1.72E-05	4.76
				qRV_CS_4.4	RV	E1	CS	1.73E-05	4.76
19	S04_14382955	14382955	4	*qRV_CS_4.5*	RV	E1	CS	1.89E-05	4.72
				qRV_CS_4.6	RV	E1	CS	1.89E-05	4.72
20	S04_14413736	14413736	4	*qDRW_CS_4.3*	DRW	E1	CS	1.71E-06	5.77

TRL=total root length, RPA=root projected area, TRSA=total root surface area, ARD =average root diameter, RV=root volume, RT= root tips, RF=root forks, RC=root crossings (RC), FSW=fresh shoot weight, DSW dry shoot weight, FRW=fresh root weight, and DRW = dry root weight. E1 = growth chamber cold stress (CS) condition and E2 = controlled (C) greenhouse condition.

S. No.	Marker ID	Marker position (bp)	chr.	QTN name	Trait name	Environment	Env name	P value	LOD score
				qRV_CS_4.7	RV	E1	CS	1.00E-06	6.00
21	S04_17948502	17948502	4	*qRPA_CS_4.3*	RPA	E1	CS	1.34E-05	4.87
				qTRL_CS_4.1	TRL	E1	CS	1.58E-05	4.80
				qTRSA_CS_4.3	TRSA	E1	CS	1.33E-05	4.88
22	S04_21555270	21555270	4	*qRF_CS_4.1*	RF	E1	CS	5.55E-05	4.26
				qRPA_CS_4.4	RPA	E1	CS	4.54E-05	4.34
				qTRL_CS_4.2	TRL	E1	CS	4.13E-05	4.38
				qTRSA_CS_4.4	TRSA	E1	CS	1.33E-05	4.88
23	S04_33155690	33155690	4	*qRC_CS_4.1*	RC	E1	CS	1.51E-05	4.82
				qRF_CS_4.2	RF	E1	CS	1.92E-05	4.72
				qRPA_CS_4.5	RPA	E1	CS	1.07E-05	4.97
				qRV_CS_4.8	RV	E1	CS	1.95E-05	4.71
				qTRL_CS_4.3	TRL	E1	CS	1.56E-05	4.81
				qTRSA_CS_4.5	TRSA	E1	CS	8.80E-05	4.06
24	S05_6875376	6875376	5	*qRPA_CS_5.1*	RPA	E1	CS	3.30E-05	4.48
				qRV_CS_5.1	RV	E1	CS	2.30E-05	4.64
				qTRSA_CS_5.1	TRSA	E1	CS	3.29E-05	4.48
25	S05_6875381	6875381	5	*qRPA_CS_5.2*	RPA	E1	CS	3.30E-05	4.48
				qRV_CS_5.2	RV	E1	CS	2.30E-05	4.64

TRL=total root length, RPA=root projected area, TRSA=total root surface area, ARD =average root diameter, RV=root volume, RT= root tips, RF=root forks, RC=root crossings (RC), FSW=fresh shoot weight, DSW dry shoot weight, FRW=fresh root weight, and DRW = dry root weight. E1 = growth chamber cold stress (CS) condition and E2 = controlled (C) greenhouse condition.

S. No.	Marker ID	Marker position (bp)	chr.	QTN name	Trait name	Environment	Env name	P value	LOD score
				qTRSA_CS_5.2	TRSA	E1	CS	3.29E-05	4.48
26	S05_6875709	6875709	5	*qRPA_CS_5.3*	RPA	E1	CS	8.12E-05	4.09
				qRV_CS_5.3	RV	E1	CS	3.62E-05	4.44
				qTRSA_CS_5.3	TRSA	E1	CS	8.09E-05	4.09
27	S05_6993912	6993912	5	*qRPA_CS_5.4*	RPA	E1	CS	8.56E-05	4.07
				qRV_CS_5.4	RV	E1	CS	3.58E-05	4.45
				qTRSA_CS_5.4	TRSA	E1	CS	8.53E-05	4.07
28	S05_6994191	6994191	5	*qRPA_CS_5.5*	RPA	E1	CS	7.44E-05	4.13
				qRV_CS_5.5	RV	E1	CS	4.94E-05	4.31
				qTRSA_CS_5.5	TRSA	E1	CS	7.41E-05	4.13
29	S05_6994476	6994476	5	*qRPA_CS_5.6*	RPA	E1	CS	7.62E-05	4.12
				qRV_CS_5.6	RV	E1	CS	5.12E-05	4.29
				qTRSA_CS_5.6	TRSA	E1	CS	7.59E-05	4.12
30	S05_7118159	7118159	5	*qRPA_CS_5.7*	RPA	E1	CS	1.20E-05	4.92
				qRV_CS_5.7	RV	E1	CS	6.90E-05	4.16
				qTRL_CS_5.1	TRL	E1	CS	4.75E-06	5.32
				qTRSA_CS_5.7	TRSA	E1	CS	1.20E-05	4.92
31	S07_924681	924681	7	*qRC_CS_7*	RC	E1	CS	6.04E-06	5.22
				qRF_CS_7.1	RF	E1	CS	7.05E-06	5.15

TRL=total root length, RPA=root projected area, TRSA=total root surface area, ARD =average root diameter, RV=root volume, RT= root tips, RF=root forks, RC=root crossings (RC), FSW=fresh shoot weight, DSW dry shoot weight, FRW=fresh root weight, and DRW = dry root weight. E1 = growth chamber cold stress (CS) condition and E2 = controlled (C) greenhouse condition.

S. No.	Marker ID	Marker position (bp)	chr.	QTN name	Trait name	Environment	Env name	P value	LOD score
				qRPA_CS_7.1	RPA	E1	CS	7.94E-05	4.1
				qTRL_CS_7.1	TRL	E1	CS	1.16E-05	4.94
				qTRSA_CS_7.1	TRSA	E1	CS	7.93E-05	4.10
32	S07_11205230	11205230	7	*qRPA_CS_7.2*	RPA	E1	CS	4.66E-05	4.33
				qRV_CS_7.1	RV	E1	CS	6.85E-05	4.16
33	S07_11475347	11475347	7	*qRPA_CS_7.3*	RPA	E1	CS	4.78E-05	4.32
				qRV_CS_7.2	RV	E1	CS	5.13E-05	4.29
				qTRSA_CS_7.2	TRSA	E1	CS	4.78E-05	4.32
34	S07_11482432	11482432	7	*qRPA_CS_7.4*	RPA	E1	CS	4.78E-05	4.32
				qRV_CS_7.3	RV	E1	CS	5.13E-05	4.29
				qTRSA_CS_7.3	TRSA	E1	CS	4.78E-05	4.32
35	S07_11482467	11482467	7	*qRPA_CS_7.5*	RPA	E1	CS	4.78E-05	4.32
				qRV_CS_7.4	RV	E1	CS	5.13E-05	4.29
				qTRSA_CS_7.4	TRSA	E1	CS	4.78E-05	4.32
36	S07_11482488	11482488	7	*qRPA_CS_7.6*	RPA	E1	CS	4.78E-05	4.32
				qRV_CS_7.5	RV	E1	CS	5.13E-05	4.29
				qTRSA_CS_7.5	TRSA	E1	CS	4.78E-05	4.32
37	S07_11482701	11482701	7	*qRPA_CS_7.7*	RPA	E1	CS	1.88E-05	4.73
				qRV_CS_7.6	RV	E1	CS	2.25E-05	4.65

TRL=total root length, RPA=root projected area, TRSA=total root surface area, ARD =average root diameter, RV=root volume, RT= root tips, RF=root forks, RC=root crossings (RC), FSW=fresh shoot weight, DSW dry shoot weight, FRW=fresh root weight, and DRW = dry root weight. E1 = growth chamber cold stress (CS) condition and E2 = controlled (C) greenhouse condition.

S. No.	Marker ID	Marker position (bp)	chr.	QTN name	Trait name	Environment	Env name	P value	LOD score
				qTRL_CS_7.2	TRL	E1	CS	4.89E-05	4.31
				qTRSA_CS_7.6	TRSA	E1	CS	1.88E-05	4.73
38	S07_25857798	25857798	7	*qDRW_CS_7.1*	DRW	E1	CS	5.53E-07	6.26
				qDRW_CS_7.6	DSW	E1	CS	1.29E-05	5.01
				qFRW_CS_7.2	FRW	E1	CS	7.84E-05	5.01
				qFSW_CS_7	FSW	E1	CS	1.69E-06	6.01
				qRF_CS_7.2	RF	E1	CS	1.27E-05	4.90
				qRPA_CS_7.8	RPA	E1	CS	5.35E-07	6.27
				qRV_CS_7.1	RV	E1	CS	3.39E-06	5.47
				qTRL_CS_7.3	TRL	E1	CS	5.34E-07	6.27
39	S07_25857799	25857799	7	*qDRW_CS_7.2*	DRW	E1	CS	5.53E-07	6.26
				qRF_CS_7.3	RF	E1	CS	1.27E-05	4.90
				qRPA_CS_7.9	RPA	E1	CS	5.35E-07	6.27
				qRV_CS_7.2	RV	E1	CS	3.39E-06	5.47
				qTRL_CS_7.4	TRL	E1	CS	1.33E-06	5.88
				qTRSA_CS_7.7	TRSA	E1	CS	5.34E-07	6.27
40	S07_25857831	25857831	7	*qDRW_CS_7.3*	DRW	E1	CS	5.89E-07	6.23
				qRF_CS_7.4	RF	E1	CS	5.65E-05	4.25
				qRPA_CS_7.10	RPA	E1	CS	3.26E-06	5.49

TRL=total root length, RPA=root projected area, TRSA=total root surface area, ARD =average root diameter, RV=root volume, RT= root tips, RF=root forks, RC=root crossings (RC), FSW=fresh shoot weight, DSW dry shoot weight, FRW=fresh root weight, and DRW = dry root weight. E1 = growth chamber cold stress (CS) condition and E2 = controlled (C) greenhouse condition.

S. No.	Marker ID	Marker position (bp)	chr.	QTN name	Trait name	Environment	Env name	P value	LOD score
				qRV_CS_7.3	RV	E1	CS	1.68E-05	4.78
				qTRL_CS_7.5	TRL	E1	CS	6.30E-06	5.20
				qTRSA_CS_7.8	TRSA	E1	CS	3.25E-06	5.49
41	S10_1362283	1362283	10	*qARD_CS_10.6*	ARD	E1	CS	5.10E-06	5.29
				qRV_CS_10.1	RV	E1	CS	6.48E-05	4.19
42	S10_1391854	1391854	10	*qARD_CS_10.7*	ARD	E1	CS	7.12E-06	5.15
				qRV_CS_10.2	RV	E1	CS	7.10E-05	4.15
43	S10_2688986	2688986	10	*qRC_C_10*	RC	E2	C	3.88E-05	4.41
				qRF_C_10	RF	E2	C	4.04E-05	4.39
44	S10_17363025	17363025	10	*qRPA_C_10.3*	RPA	E2	C	2.26E-05	4.65
				qTRL_C_10	TRL	E2	C	1.01E-04	4.00
45	S10_20894121	20894121	10	*qRPA_CS_10*	RPA	E1	CS	1.00E-04	4
				qRV_CS_10.3	RV	E1	CS	1.26E-05	4.90
				qTRSA_CS_10	TRSA	E1	CS	1.01E-04	4.00
46	S11_6628302	6628302	11	*qRC_CS_11.1*	RC	E1	CS	8.41E-05	4.08
				qRF_CS_11.1	RF	E1	CS	8.63E-05	4.06
				qTRL_CS_11.1	TRL	E1	CS	9.14E-05	4.04
47	S11_9489484	9489484	11	*qRC_CS_11.2*	RC	E1	CS	3.43E-05	4.46
				qRF_CS_11.2	RF	E1	CS	4.83E-05	4.32

TRL=total root length, RPA=root projected area, TRSA=total root surface area, ARD =average root diameter, RV=root volume, RT= root tips, RF=root forks, RC=root crossings (RC), FSW=fresh shoot weight, DSW dry shoot weight, FRW=fresh root weight, and DRW = dry root weight. E1 = growth chamber cold stress (CS) condition and E2 = controlled (C) greenhouse condition.

S. No.	Marker ID	Marker position (bp)	chr.	QTN name	Trait name	Environment	Env name	P value	LOD score
48	S11_24102290	24102290	11	*qRC_CS_11.3*	RC	E1	CS	5.64E-05	4.25
				qRF_CS_11.3	RF	E1	CS	9.17E-05	4.04
49	S11_29386484	29386484	11	*qRPA_CS_11*	RPA	E1	CS	8.96E-05	4.05
				qRV_CS_11	RV	E1	CS	7.74E-05	4.11

TRL=total root length, RPA=root projected area, TRSA=total root surface area, ARD =average root diameter, RV=root volume, RT= root tips, RF=root forks, RC=root crossings (RC), FSW=fresh shoot weight, DSW dry shoot weight, FRW=fresh root weight, and DRW = dry root weight. E1 = growth chamber cold stress (CS) condition and E2 = controlled (C) greenhouse condition.

Identification of candidate genes

A total of 49 multi-trait loci were subjected to candidate gene analysis, within which 74 putative candidate genes with known functions were identified across 24 genetic loci (Table S2). Candidate genes were retrieved from the RAP-DB database using a 100-kb window upstream and downstream of each target locus. The locus S01_25632084, which contained two QTNs (*qRPA_C_1* and *qTRL_C_1.1*) under E2 (Table 2), harbored the highest number of candidate genes (n = 7): *Os01g0639900*, *Os01g0637800*, *Os01g0637600*, *Os01g0637500*, *Os01g0639100*, *Os01g0639200*, and *Os01g0638600*, corresponding to the well-characterized genes *OsβCA1*, *OsMYB305*, *OsPDF1B*, *OsPG3*, *OsRH2*, *Snl6*, and *UGT703A1*, respectively (Table S2). Under E1, six genes were identified in each genetic locus including S02_23143820 (*Os02g0594800*, *Os02g0596300*, *Os02g0596200*, *Os02g0595900*, *Os02g0594700*, and *Os02g0595700*), S04_33155690 (*Os04g0650000*, *Os04g0650300*, *Os04g0650800*, *Os04g0649100*, *Os04g0652400*, and *Os04g0649400*), and S10_20894121 (*Os10g0537800*, *Os10g0537600*, *Os10g0536100*, *Os10g0536400*, *Os10g0536000*, and *Os10g0536150*). S07_25857798 genetic loci was associated with eight multi traits (Table 2), which identified potential genes as *Os07g0622900*, *Os07g0623100*, *Os07g0623200*, *Os07g0623300*, *Os07g0623400*, and *Os07g0624600*, which corresponds to well-known genes *DTM1*, *OsCAMTA3*, *OsHMA7*, *OsSC32*, *OsSPT4*, and *OsTPP3*, respectively. Many of the identified genes are involved in plant growth and development, tolerance to biotic and abiotic stresses, grain development, pollen viability, nutrient uptake, and overall plant adaptation (Table S2). Several key genes were identified, including *OsNIP1;2*, associated with aluminum tolerance; *OsNAR2.1* and *OsMYB305*, involved in nitrogen uptake; *OsPP2C27*, a negative regulator of CT; *MHZ11*, which regulates ethylene signaling in rice roots; and *OsDWARF*, which controls brassinosteroid biosynthesis and thereby influences root growth (Table S2).

Discussion

RSA is a complex, polygenic trait regulated by numerous genes [4, 46]. Root-focused studies are essential for improving CT as roots are highly sensitive to CS and play a central role in plant survival and recovery. Integrating CS responses with root developmental and genetic analyses provides a molecular basis for breeding root traits that enhance adaptation under LT conditions [47]. CS often leads to altered root anatomical traits such as changes in cortex thickness and vascular bundle development, which influence nutrient and water uptake capacity [48]. CS disrupts root metabolism, plant morphology, and seedling structure through anatomical, physiological, and biochemical alterations in rice [5]. Soil temperature strongly regulates root growth, with both excessively low and high

temperatures inhibiting root system development [49–51]. Given the sensitivity of rice roots to temperature, this study aims to dissect the genetic basis of RSA under both CS and optimal conditions using a diverse rice germplasm panel, thereby identifying loci that specifically regulate root adaptation to cold.

Phenotypic variation provides a strong foundation for genetic dissection of complex traits like RSA, to improve root performance under different temperature regimes (Fig. 1). RSA study traits showed continuous distribution across environments (Fig. 2), indicating broad diversity available in root growth and architecture traits in this diverse germplasm panel. The descriptive statistics (Table 1) showed that RSA and biomass traits were significantly affected by the temperature regime, indicating that CS imposed a strong environmental constraint on root growth and whole-plant performance. Earlier reports also suggested that low root-zone temperature suppresses rice root development and alters seedling physiology and morphology, ultimately reducing biomass accumulation [5, 51]. The large genotype-dependent variation in RSA and biomass traits across stress and non-stress conditions (Table 1) indicates strong root phenotypic plasticity and the presence of exploitable allelic diversity for stress adaptation in rice [52, 53]. This combination of broad phenotypic range with measurable genetic control (h^2) provides sufficient signal to support GWAS, enabling detection of loci underlying both baseline root development and stress-responsive root remodeling [54, 55]. The variance components indicate that temperature regime strongly modulated the genetic control of RSA and biomass traits, with several traits showing moderate heritability under E1 (TRL, DSW, and FRW h^2 was 0.63, 0.55, and 0.49, respectively) but generally lower heritability under E2, consistent with evidence that low/root-zone temperature reshapes rice root development and associated physiology mechanism [56–58]. In the pooled analysis, higher heritability for traits such as TRL (h^2=0.88), FSW (h^2=0.72), and RT (h^2=0.60) suggests comparatively stable genotype effects across environments, whereas lower pooled h^2 for other traits likely reflects increased environmental sensitivity and genotype × environment interactions typical for root traits under temperature stress [59, 60].

Higher CVs for RT, RF, RC, and FSW indicate strong environmental sensitivity and high phenotypic plasticity, whereas ARD showed relatively stable expression (Table 1). The consistently high pooled CV further reflects pronounced environmental modulation and genotype × environment effects, supporting the need to evaluate RSA across contrasting conditions for robust genetic inference [61]. The pooled analysis showed higher CV values because trait means differed markedly between the two contrasting environments, inflating overall dispersion when data were combined [62]. However, the pooled heritability remained moderate to high for several traits, indicating that genotype effects were still strong and consistent across conditions despite environmental variation. RSA traits were highly correlated, shared QTNs across traits may partly reflect correlated phenotypes rather than fully independent genetic effects. Therefore, we refer these loci as multi-trait associated loci, acknowledging that further validation is needed to confirm true pleiotropic action. Earlier reports in maize showing that CS restricts root growth, yet genetic factors strongly govern root developmental plasticity and post-stress recovery, making root length a key indicator of CT [54]. The moderate-to-high heritability of TRL under CS therefore supports its use as a reliable selection target in future for rice breeding CT genotypes, and the strong TRL phenotypic correlations among root traits across both environments further indicate coordinated genetic regulation of RSA.

GWAS provides an efficient approach for dissecting genetic variation underlying multiple traits in rice [22, 23, 63, 64]. GWAS has been successfully applied to identify genomic regions associated with CS tolerance in faba bean by detecting significant QTLs controlling root traits under LT conditions [28]. In recent years, numerous GWAS studies have successfully investigated for CT during germination, seedling-stage, and shoot traits in rice [22, 24, 65–68]. To date, no GWAS has reported root trait associations in rice under CS and in this study we identified 143 QTNs for RSA traits across two environments (Table S1). Earlier biparental mapping studies identified 40 QTLs controlling root weight, length, and diameter of primary and seminal roots in maize seedlings under CS [69]. In this study, GWAS was

performed using BLUE values and the FarmCPU model implemented in the rMVP package in R [45]. This method reduces false positives and makes it especially effective for detecting complex, polygenic traits like RSA. In our study, Manhattan plots displayed significant genomic associations, while Q-Q plots evaluated model fit and control of false positives (Fig. S1-S6). The significant higher number of QTNs detected under CS (E1; 87 QTNs) compared with control conditions (E2; 56 QTNs) indicates that rice RSA is governed by a distinct and more complex genetic network during stress. This emphasizes the importance of stress-specific GWAS for uncovering loci that are directly involved in cold adaptation and would otherwise remain undetected under optimal conditions. Numerous GWAS have mapped QTLs controlling rice RSA under normal seedling conditions, including studies in *japonica* and *indica* diverse accessions, Vietnamese varieties, and large panels such as the 3K RGP [29–34]. These studies revealed loci for root length, dry weight, and branching, highlighting the complex genetic control of RSA. However, most of these studies were conducted under optimal growth conditions or other stresses, and none of explored root trait variation under CS in rice, understanding the need for stress-specific GWAS to uncover loci involved in cold adaptation.

Multi-trait QTNs are regulated by multiple traits through shared genetic pathways, allowing simultaneous improvement of root architecture and stress tolerance. Such multi-trait loci have been widely reported as genetic hubs controlling coordinated phenotypic responses and are ideal targets for breeding for complex traits [70, 71]. The high number of multi-traits QTNs detected under CS (45 in E1 and only 4 in E2), indicates that RSA are governed by tightly coordinated genetic networks that are strongly activated under CS conditions (Table 2). The highest multi-trait loci were located on chromosomes 3 and 7 (n = 10 each) with major locus S07_25857798 controlling eight root traits (DRW, DSW, FRW, FSW, RF, RPA, RV, and TRL) suggesting these genomic regions as key genetic hubs for cold-responsive root architecture. The genetic loci S04_33155690, S07_25857799, and S07_25857831 exhibited strong multi-trait loci effects, each being associated with six root traits, including combinations of root traits including RFW, RDW, RPA, RV, TRL, and TRSA. Such multi-trait loci represent promising targets for breeding strategies aimed at simultaneously improving multiple root traits to enhance multi-stress tolerance including CT [5, 46]. Among the multi-trait loci, TRL is a key trait for CT as it enhances water and nutrient uptake, supports seedling establishment, and maintains root system function under LT stress. In rice, longer roots correlate with improved cold resilience at the seedling stage [5, 48], while in maize and wheat, increased TRL under LT or drought conditions has been linked to better stress adaptation and higher survival [72, 73]. Overall findings suggest TRL as a key phenotypic and breeding target for improving abiotic stress tolerance across crops.

The co-localization of 25 QTNs with previously reported RSA loci under normal, salt, and drought conditions suggests that parts of the root genetic architecture are shared across multiple environments and stresses, reflecting stable and conserved regulatory pathways (Table S1). QTNs detected under CS (14 in E1) may represent robust loci with broader stress relevance, whereas those detected in the control (11 in E2) likely capture baseline root development effects. The loci S01_25632084 and S01_25766658 co-localized with *qi01-1*, a QTL previously reported for root cone angle under normal growth chamber conditions [74]. S07_15182004 and S07_15182022 associated with FSW under CS corresponded to *qRTW3*, a QTL linked to total root length under normal growth [75]. Several multi-trait loci detected under CS; S05_6875376, S05_6875381, S05_6875709, S05_6993912, S05_6994191, S05_6994476, and S05_7118159, co-localized with root growth ability loci reported under normal conditions [31]. Likewise, S03_26735628 carrying *qFRW_C_3.2* overlapped with *qMRL3.2*, which controls main root length under normal conditions [32]. S02_20226093 identified two QTNs (*qRPA_C_2* and *qTRL_C_2*) that overlapped with the previously reported locus *SNP2-63635110* associated with root fork number under salt stress, whereas S02_23143820 contained three QTNs (*qRPA_CS_2.1*, *qRV_CS_2.1*, and *qTRSA_CS_2.1*) co-localized with *SNP2-66495205* linked to root length under salt stress [76]. Importantly, the remaining non-overlapping QTNs may represent novel cold-responsive loci, providing new targets for improving RSA under CS. Going forward, the co-localized QTNs can be exploited as

stable RSA loci for breeding, while the cold-specific QTNs should be explored as temperature-responsive targets through multi-environment validation and candidate gene functional analysis.

Candidate genes approach allows the detection of potential known genes regulating multiple root traits and which conserved genomic regions that may underline coordinated root responses across different environments. To identify candidate genes, multi-trait loci from both environments were examined using a 100-kb window upstream and downstream of the target QTN positions, following approaches successfully applied in previous studies [22, 23, 77, 78]. A total of 74 putative candidate genes with known functions were identified across 24 genetic loci from RAP-DB platform (Table S2). Although 49 multi-trait QTNs were examined, well-annotated candidate genes were detected at only 24 loci, likely reflecting incomplete genome annotation, the prevalence of regulatory variants, extended LD, and the contribution of novel or cold-responsive genes that remain functionally uncharacterized. Under E2, the locus S01_25632084, contained the highest number of candidate genes, corresponding to well-characterized genes involved in nutrient uptake, development of chloroplast and mitochondria, regulating plant height, pollen and seed development, including *OsβCA1*, *OsMYB305*, *OsPDF1B*, *OsPG3*, *OsRH2*, *Snl6*, and *UGT703A1* (Table S2). The *OsMYB305* (*Os01g0637800*) gene functions as a transcriptional activator that enhances nitrogen uptake and root nutrient signaling under low-nitrogen conditions and plays a positive role in alkalinity tolerance at the seedling stage [79, 80]. Its involvement in regulating nutrient transporters and ion homeostasis suggests a potential role in coordinating root metabolic and adaptive responses under stress conditions. In contrast, under E1, several loci including S02_23143820, S04_33155690, and S10_20894121 each contained six candidate genes, reflecting a more distributed genetic control of root traits under CS (Table S2). *Os02g0596300*, encoding a cytochrome P450 enzyme, belongs to a large gene family in rice involved diverse biological function, including hormone biosynthesis and signaling, and plays key roles in regulating plant growth, root development, and tolerance to biotic and abiotic stresses such as cold, drought, heat, and salinity through modulation of stress-related metabolic and signaling networks [81–87].

The locus S02_23143820 harbored three QTNs (*qRPA_CS_2.1*, *qRV_CS_2.1*, and *qTRSA_CS_2.1*), within which the gene *EF-Tu* (*Os02g0595700*) was identified. *EF-Tu* has been reported to play a crucial role in chloroplast development under LT conditions in rice [88], heat tolerance in maize and wheat [89, 90], highlighting its conserved role in temperature stress adaptation across cereal crops. Another gene in the same genomic region identified as *OsNAR2.1* (*Os02g0595900*) is highly relevant, as it functions as a key partner protein and activator of *NRT2* nitrate transporters, enabling high-affinity nitrate uptake across a different level of nitrogen and regulating root growth responses to nitrate and ammonium. Moreover, *OsNAR2.1* integrates nutrient signaling with stress adaptation by modulating, TFs activity and enhancing drought tolerance and grain yield, underscoring its potential role in coordinating nutrient acquisition and root development under abiotic stress conditions [91–96]. The locus S05_6993912 contained three QTNs (*qRPA_CS_5.4*, *qRV_CS_5.4*, and *qTRSA_CS_5.4*) and harbored the candidate gene *Os05g0213500*, corresponding to *OsPYL/RCAR5* (*PYL5*), a key regulator of ABA signal transduction. *PYL5* plays an important role in abiotic stress tolerance by regulating seed germination and early seedling growth and by enhancing drought tolerance, highlighting its potential involvement in ABA-mediated root responses under stress condition [97, 98]. The association of *OsPP2C27* (*Os02g0799000*) with multiple root traits (RPA, RV and TRSA) highlights its multi-trait loci role in regulating root architecture under CS. As a negative regulator of CT, *OsPP2C27* modulates stress signaling by dephosphorylating *OsMAPK3*, *OsbHLH002*, and *OsWRKY7*, thereby influencing root growth and stress balance during early rice seedling development [99, 100]. These multi-trait loci highlight that rice root traits under CS are regulated by nutrient uptake, ABA signaling, and stress-response pathways that maintain root growth and function.

Remarkably, the multi-trait locus S07_25857798, associated with eight root-related traits (Table 2), emerged as a major genetic hub for cold-responsive RSA by harboring six functionally important genes *DTM1*, *OsCAMTA3*,

OsHMA7, *OsSC32*, *OsSPT4*, and *OsTPP3* (Table S2). *DTM1* (*Os07g0622900*) encodes a cereal-specific endoplasmic reticulum membrane protein essential for early tapetum development and meiosis [101], suggesting a broader role in cellular integrity under stress. *OsCAMTA3* (*Os07g0623100*), a calmodulin-binding transcriptional activator, is involved in calcium-mediated signaling and negatively regulates rice blast resistance [102], emphasizing its role in stress signaling crosstalk. *OsHMA7* (*Os07g0623200*), a heavy metal ATPase, has been reported to exert strong multi-trait effects on plant architecture and grain Fe/Zn accumulation [103], indicating potential links between nutrient homeostasis and root performance. *OsSPT4* (*Os07g0623400*) contributes to pollen viability and overall plant growth and development [104], while *OsTPP3* (*Os07g0624600*) is a well-characterized regulator of seed germination under LT and tolerance to drought and salinity stresses [105–107]. Collectively, these genes reveal the multifunctional nature of this locus and its pivotal role in coordinating root development and stress adaptation under cold conditions.

The locus S01_5704110 contributed four QTNs (*qDRW_CS_1*, *qRPA_CS_1*, *qRV_CS_1*, and *qTRSA_CS_1*), within which *OsNIP1;2* (*Os01g0202800*), a nodulin 26-like intrinsic protein, was identified (Table S2). *OsNIP1;2* plays a key role in aluminum tolerance in rice by mediating internal aluminum detoxification through removal of aluminum from the root cell wall and its sequestration and redistribution within plant tissues [108]. Its root-specific induction under aluminum stress highlights its importance in maintaining root function under acidic soil conditions. We also identified *OsSWEET3a* (*Os05g0214300*) gene which supports to root development indirectly by regulating sugar and gibberellin transport, ensuring adequate energy supply and hormonal balance required for root cell division, elongation, and early seedling establishment in rice [109]. By coordinating carbon allocation and gibberellin signaling, *OsSWEET3a* helps maintain root growth and vigor, especially during early developmental stages and stress conditions. Additionally, we identified *SGW5* (*Os02g0543400*), a well characterized gene which positively regulates the grain size by WRKY53 TFs in rice [110]. Together, these genes indicate that CS responsive root traits in rice are governed by detoxification, carbon hormone transport, and multi-trait loci links to yield-related traits.

The locus S03_22599359 harbored two QTNs (*qRV_CS_3.4* and *qTRL_CS_3.3*) under E1, within which *Os03g0602300* was identified as the well-characterized genes *OsBRD1/OsDWARF*, involved in brassinosteroid biosynthesis and this gene plays a crucial role in regulating plant architecture and root growth in rice [111, 112]. The locus S05_6875376 was associated with three QTNs (*qRPA_CS_5.1*, *qRV_CS_5.1*, and *qTRSA_CS_5.1*) and identified as *Os05g0210100* (*MHZ11*) gene, a GDSL-type lipase localized to the endoplasmic reticulum. *MHZ11* regulates root growth at the seedling stage by modulating ethylene signaling through sterol homeostasis and downstream signaling components, thereby controlling ethylene-responsive root development [113, 114]. The locus S10_1362283 was associated with two QTNs (*qARD_CS_10.6* and *qRV_CS_10.1*) and well-known gene identified *OsSNDP1* (*Os10g0122600*), Sec14-nodulin domain-containing phosphatidylinositol transfer protein essential for root hair elongation through regulation of phospholipid signaling and membrane dynamics [115]. Root hairs play a critical role in integrating hormone signaling pathways (auxin, jasmonate, ethylene, and cytokinin) and ROS responses under CS, as reported in wheat and maize [116, 117]. Overall, these pathways contribute to maintaining root growth, architecture, and signaling capacity under LT conditions in rice.

Collectively, the identified genes are implicated in plant growth and development, stress tolerance, grain development, pollen viability, nutrient uptake, and overall plant adaptation, underscoring their potential relevance for improving CT through root system optimization.

Conclusion

We observed significant phenotypic variation across multiple RSA traits under both environments, indicating the polygenic nature and environmental influence these traits. GWAS identified 143 significant QTNs across both

environments, including 25 that overlapped with previously reported root-trait loci detected under normal, salt, and drought conditions. In addition, 49 QTNs showed multi-trait effects and were prioritized for candidate gene analysis. A total of 74 putative candidate genes were identified, including several well characterized know genes. Several key candidate genes were highlighted, including *OsBRD1/OsDWARF* (brassinosteroid biosynthesis supporting root growth), *MHZ11* (ethylene signaling regulating root growth), *OsSNDP1* (phospholipid-dependent root hair development), *OsPP2C27* (a negative regulator of CT), *OsNIP1;2* (aluminum tolerance), *OsNAR2.1* and *OsMYB305* (nitrogen uptake, with *OsMYB305* also linked to salinity tolerance), *OsSWEET3a* (supporting root growth and vigor under stress), and *OsHMA7* (a heavy metal ATPase influencing plant architecture and grain Fe/Zn accumulation), collectively emphasis the genetic pathways underlying stress-responsive root development in rice. These findings advance our understanding of the genetic control of RSA and its regulation under CS, and they highlight promising targets for improving root architecture and enhancing stress tolerance in rice breeding programs.

Material and methods

Experimental design

A set of 204 diverse rice germplasms, including *indica* and *japonica* cultivars, landraces, and inbred lines [22, 35], were screened at the Texas A&M AgriLife Research and Extension Center at Beaumont, TX, USA in 2023 for RSA traits. The experiment was conducted under two environmental conditions, growth chamber cold condition (E1), and controlled greenhouse condition (E2). The duration of experiment was four weeks in both environments. The E1 and E2 experiments were performed from March 3 to April 1, and from May 12 to June 9, respectively following Randomized Complete Block Design, in two replications. For each replication, 15 seeds per accession were planted in E1, whereas 30 seeds per accession were planted in E2. Immediately after planting, the germination trays were kept in the greenhouse for the first 48 h for a homogeneous start of the germination in both experiments, when the temperatures remained between 28–30°C (night/day). After 48 h of the germination start period, the trays were shifted to the growth chamber cold condition for E1. The trays were continuously kept in the greenhouse for the E2 environmental condition. In E1, the average day/night temperature of the first and second weeks was maintained at 10^{o}C, followed by 17^{o}C in the third and fourth weeks, while in E2, the overall average night and day temperature remained between 28-30^{o}C throughout the experiment. For both experiments, germination trays were filled with field soil to ensure the same field conditions throughout the experiment.

Phenotyping for RSA traits

Four weeks after planting, three seedlings from each replication were carefully harvested for root sampling. Excess soil and moisture were gently removed to minimize the risk of microbial decay. The roots were then immediately stored in Ziploc bags containing 70% ethanol and kept at 4°C for subsequent phenotypic analysis of RSA. A total of 2448 roots were harvested across both experiments. At the time of sampling, all three seedlings fresh shoot and root weight was recorded, followed by measurements of their dry weights after drying at 65°C for 72 h. All roots were scanned using a flatbed scanner (Epson perfection V700 photo, Nagano, Japan) equipped with the WinRHIZO Pro software package (Regent Instruments Inc., Quebec, Canada). WinRHIZO Pro (version 23a) was used to analyze root morphology, which provided data on total root length (TRL, cm), root projected area (RPA, cm^2), total root surface area (TRSA, cm^2), average root diameter (ARD, mm), root volume (RV, cm^3), root tips (RT), root forks (RF), and root crossings (RC). Additionally, data were collected for fresh shoot weight (FSW, g), dry shoot weight (DSW, g), fresh root weight (FRW, g), and dry root weight (DRW, g).

Phenotyping data analysis

BLUEs (Best Linear Unbiased Estimates) values were calculated from E1 and E2 of each trait for each genotype using the “lme4” package in R 4.4.2 [36]. BLUEs were estimated to be using linear mixed models in the lme4 package [37], considering genotype as a fixed effect and replication as random effects following standard mixed-model approaches [38, 39]. Analysis of variance (ANOVA) was performed in RCBD design using the “agricolae” package in R studio software v4.3.1 [40]. Broad-sense heritability (h^2) for each trait was calculated under both environments [41], using following formula.

$$h^2 = \frac{Vg}{Vg + Ve/R}$$

Where, h^2 is the broad-sense heritability, Vg is the genetic variance, Ve error variance, R is the number of replications. Correlations among the different traits were evaluated using Pearson’s correlation coefficients in R studio software v4.3.1 using the “corrplot” package [40].

Genotyping and population structure

The population was genotyped using the genotyping-by-sequencing approach at Texas A&M AgriLife Genomics and Bioinformatics Service (TxGen), College Station, TX, USA and the genomic data were obtained from previously published studies [22, 35]. In brief, BEAGLE V4.0 software [42] was used to remove all SNP markers (1,075,302) with more than 50% missing data and a minimum allele frequency (MAF) of < 0.05 across genotypes. Markers were imputed and filtered using TASSEL 5.2.61 [43], removing SNPs with low-quality clustering and MAF < 0.05. After that, 854,832 SNPs were chosen and utilized for the GWAS analysis. The marker data is available on Dryad (https://datadryad.org/dataset/doi:10.5061/dryad.4qrfj6qbs) [35]. Population structure and linkage disequilibrium (LD) analyses were conducted following the procedures described in previous studies where the same population was used [22, 35].

Genome-wide association analysis

The GWAS analysis was performed using BLUEs value data from all the 12 traits studied. A total of 854,832 SNPs were analyzed for genome-wide associations using the fixed and random model circulating probability unification (FarmCPU) [44] within the ‘rMVP’ package [45] in R. FarmCPU in rMVP provides a high statistical power with strong control of false discoveries, population structure, and is computationally efficient for large-scale SNP datasets, making it well suited for multi-trait GWAS using BLUEs. Manhattan and quantile-quantile (QQ) plots were generated using the “CMplot” R package (https://github.com/YinLiLin/R-CMplot). LOD score > 4.0 (P value 1×10^{-4}) was used to declare significant QTNs (quantitative trait nucleotides) in both environments.

Identification of candidate genes

QTNs (marker sequences) associated with more than two RSA traits were used for candidate gene analysis in RAP-BD database (https://rapdb.dna.affrc.go.jp/search/). The searches were performed with default parameters to identify putative candidate genes located in proximity to these QTNs. Genes within each locus were identified using the physical locations of the SNP marker's upstream and downstream of 100 kb. Based on RAP-DB gene symbol synonyms, gene functions were verified, and only well-characterized genes were retained.

Declarations

Funding

This work was supported by the Texas Rice Research Foundation and Texas A&M AgriLife Research.

Author Contribution

SKT, GS, and SM conceptualized and designed the experiments. RYS, CH, and GS collected root samples from both experiments and extracted data using WinRHIZO Pro software. SM, RI, SDJ, SKD, and ILVG assisted GS with data analysis, interpretation of results, and preparation of the first draft of the manuscript. GS, RI, SDJ, SKD, and ILVG critically revised and edited the manuscript. SKT supervised the study and finalized the manuscript. All authors have read and agreed to the final version of the manuscript.

Acknowledgement

We acknowledge the Texas Rice Research Foundation (TRRF) and Texas A&M AgriLife Research for their continued support in funding and facilitating this research.

Data Availability

All data generated or analyzed during this study are included in this published article and its supplementary information files. List of 204 genotypes is available in previously published article (Singh et al., 2025: doi.org/10.1016/j.stress.2024.100707). The genotypic data is available on Dryad (https://datadryad.org/dataset/doi:10.5061/dryad.4qrfj6qbs).

References

1. Singh, G. et al. 2Gs and plant architecture: breaking grain yield ceiling through breeding approaches for next wave of revolution in rice (Oryza sativa L). *Crit. Rev. Biotechnol.* **44**, 139–162 (2024).
2. Kaur, R. et al. Precision breeding strategy to enrich iron and zinc in rice. *Cereal Res. Commun* 1–32 (2025).
3. Bakala, H. S., Singh, G. & Srivastava, P. Smart breeding for climate resilient agriculture. in *In Plant breeding-current and future views* (2020).
4. Singh, G. et al. Omics-based approaches for decoding root dynamics in legumes. *Curr Plant. Biol* 100608 (2026).
5. Rativa, A. G. S. et al. Root responses of contrasting rice genotypes to low temperature stress. *J. Plant. Physiol.* **225**, 153307 (2020).
6. Hsu, C. H. & Hsu, Y. T. Biochemical responses of rice roots to cold stress. *Bot. Stud.* **60**, 14 (2019).
7. Xu, X. et al. Genome-wide association study of rice rooting ability at the seedling stage. *Rice* **13**, 59 (2020).
8. Mahender, A., Anandan, A. & Pradhan, S. K. Early seedling vigour, an imperative trait for direct-seeded rice: an overview on physio-morphological parameters and molecular markers. *Planta* **241**, 1027–1050 (2015).
9. Manasa, L., Panigrahy, M., Panigrahi, K. C. & Rout, G. R. Overview of cold stress regulation in plants. *Bot. Rev.* **88**, 359–387 (2022).
10. Bhattacharya, A. Effect of low-temperature stress on germination, growth, and phenology of plants: A review. *Physiol Process. plants under low Temp. Stress* **1–106** (2022).

11. Li, Z., Qiu, Z., Ge, H. & Du, C. Long-term dynamic of cold stress during heading and flowering stage and its effects on rice growth in China. *Atmos. (Basel)*. **13**, 103 (2022).
12. Shi, Y. et al. Effects of chilling at different growth stages on rice photosynthesis, plant growth, and yield. *Environ. Exp. Bot.* **203**, 105045 (2022).
13. Hu, Q. et al. Abnormal anther development leads to lower spikelet fertility in rice (Oryza sativa L.) under high temperature during the panicle initiation stage. *BMC Plant. Biol.* **21**, 428 (2021).
14. Cruz, R. P. D. et al. Avoiding damage and achieving cold tolerance in rice plants. *Food energy Secur.* **2**, 96–119 (2013).
15. Yang, X. et al. Moderate Cold Stress Enhance Drought Resistance through CCA1 via-an ABA-independent Pathway. *bioRxiv* 1–53 (2024).
16. Xiang, Z. et al. OsNCED5 confers cold stress tolerance through regulating ROS homeostasis in rice. *Plant. Physiol. Biochem.* **220**, 109455 (2025).
17. Shahzad, N., Nabi, H. G., Qiao, L. & Li, W. The molecular mechanism of cold-stress tolerance: Cold responsive genes and their mechanisms in rice (Oryza sativa L). *Biology (Basel)*. **13**, 442 (2024).
18. Byun, M. Y. et al. Identification of rice genes associated with enhanced cold tolerance by comparative transcriptome analysis with two transgenic rice plants overexpressing DaCBF4 or DaCBF7, isolated from Antarctic flowering plant Deschampsia antarctica. *Front. Plant. Sci.* **9**, 601 (2018).
19. Gu, Y. et al. QTL mapping by GWAS and functional analysis of OsbZIP72 for cold tolerance at rice seedling stage. *Crop J.* **12**, 1697–1708 (2024).
20. Gu, S. et al. Multi-omics approach reveals the contribution of OsSEH1 to rice cold tolerance. *Front. Plant. Sci.* **13**, 1110724 (2023).
21. Singh, G. et al. GWAS reveals novel QTLs associated with panicle architecture traits in US long-grain rice. *Crop Sci.* **66**, e70250 (2026).
22. Singh, G. et al. Deciphering the genomic regions associated with seedling cold tolerance traits in rice (Oryza sativa L). *Plant. Stress*. **15**, 100707 (2025).
23. Singh, G. et al. Genomic regions associated with flag leaf and panicle architecture in rice (Oryza sativa L). *BMC Genom.* **25**, 1200 (2024).
24. Rastogi, K., Mankar, S. P. & Septiningsih, E. M. Genome-wide association study for traits related to cold tolerance and recovery during seedling stage in rice. *Crop Sci.* **65**, e70003 (2025).
25. Shi, H. et al. Identification of candidate genes for cold tolerance at seedling stage by GWAS in rice (Oryza sativa L). *Biology (Basel)*. **13**, 784 (2024).
26. Khatab, A. A. et al. Global identification of quantitative trait loci and candidate genes for cold stress and chilling acclimation in rice through GWAS and RNA-seq. *Planta* **256**, 82 (2022).
27. Li, C. et al. Identification of cold tolerance QTLs at the bud burst stage in 211 rice landraces by GWAS. *BMC Plant. Biol.* **21**, 542 (2021).
28. Sallam, A., Moursi, Y. S., Martsch, R. & Eltaher, S. Genome-wide association mapping for root traits associated with frost tolerance in faba beans using KASP-SNP markers. *Front. Genet.* **13**, 907267 (2022).
29. Courtois, B. et al. Genome-wide association mapping of root traits in a japonica rice panel. *PLoS One*. **8**, e78037 (2013).
30. Phung, N. T. P. et al. Genome-wide association mapping for root traits in a panel of rice accessions from Vietnam. *BMC Plant. Biol.* **16**, 64 (2016).

31. Xu, X. et al. Genome-wide association study of rice rooting ability at the seedling stage. *Rice* **13**, 9 (2020).
32. Xiang, J. et al. Genome-wide association study reveals candidate genes for root-related traits in rice. *Curr. Issues Mol. Biol.* **44**, 4386–4405 (2022).
33. Klinsawang, S. et al. Genome-wide association study identifies key F-box genes linked to ethylene responsiveness and root growth in rice (Oryza sativa L). *Front. Plant. Sci.* **15**, 1501533 (2024).
34. das Chagas, G. B. et al. Genome-wide association study identifies loci and candidate genes for root traits in rice grown in Brazil. *Crop Des.* **4**, 100095 (2025).
35. Sanchez, D. L. et al. Phenotypic variation and genome-wide association studies of main culm panicle node number, maximum node production rate, and degree-days to heading in rice. *BMC Genom.* **23**, 390 (2022).
36. Alvarado, G. et al. META-R: A software to analyze data from multi-environment plant breeding trials. *Crop J.* **8**, 745–756 (2020).
37. Bates, D., Mächler, M., Bolker, B. & Walker, S. Fitting linear mixed-effects models using lme4. *J. Stat. Softw.* **67**, 1–48 (2015).
38. Piepho, H. P. & Mohring, J. Computing heritability and selection response from unbalanced plant breeding trials. *Genetics* **177**, 1881–1888 (2007).
39. Bernardo, R. *Breeding for Quantitative Traits in Plants*. (2002).
40. Team, R. C. RA language and environment for statistical computing, R Foundation for Statistical. *Computing* (2013).
41. Hill, W. G. & Mackay, T. F. DS Falconer and Introduction to quantitative genetics. *Genetics* **167**, 1529–1536 (2004).
42. Browning, S. R. & Browning, B. L. Rapid and accurate haplotype phasing and missing-data inference for whole-genome association studies by use of localized haplotype clustering. *Am. J. Hum. Genet.* **81**, 1084–1097 (2007).
43. Bradbury, P. J. et al. TASSEL: software for association mapping of complex traits in diverse samples. *Bioinformatics* **23**, 2633–2635 (2007).
44. Liu, X., Huang, M., Fan, B., Buckler, E. S. & Zhang, Z. Iterative usage of fixed and random effect models for powerful and efficient genome-wide association studies. *PLoS Genet.* **12**, e1005767 (2016).
45. Yin, L. et al. rMVP: a memory-efficient, visualization-enhanced, and parallel-accelerated tool for genome-wide association study. *Genomics Proteom. Bioinf.* **19**, 619–628 (2021).
46. Wachsman, G., Sparks, E. E. & Benfey, P. N. Genes and networks regulating root anatomy and architecture. *New. Phytol*. **208**, 26–38 (2015).
47. Alahakoon, D. & Fennell, A. Genetic analysis of grapevine root system architecture and loci associated gene networks. *Front. Plant. Sci.* **13**, 1083374 (2023).
48. Cheong, B. E. et al. The effect of cold stress on the root-specific lipidome of two wheat varieties with contrasting cold tolerance. *Plants* **11**, 1364 (2022).
49. González-García, M. P. et al. Temperature changes in the root ecosystem affect plant functionality. *Plant Commun* **4**, (2023).
50. Zhu, J. et al. Low temperature inhibits root growth by reducing auxin accumulation via ARR1/12. *Plant. Cell. Physiol.* **56**, 727–736 (2015).
51. Arai-Sanoh, Y., Ishimaru, T., Ohsumi, A. & Kondo, M. Effects of soil temperature on growth and root function in rice. *Plant. Prod. Sci.* **13**, 235–242 (2010).

52. Uga, Y. et al. Control of root system architecture by DEEPER ROOTING 1 increases rice yield under drought conditions. *Nat. Genet.* **45**, 1097–1102 (2013).
53. Courtois, B. et al. Rice root genetic architecture: meta-analysis from a drought QTL database. *Rice* **2**, 115–128 (2009).
54. Zhou, Y. et al. Cold mediates maize root hair developmental plasticity via epidermis-specific transcriptomic responses. *Plant. Physiol.* **196**, 2105–2120 (2024).
55. Zhao, K. et al. Genome-wide association mapping reveals a rich genetic architecture of complex traits in Oryza sativa. *Nat. Commun.* **2**, 467 (2011).
56. Gong, W. et al. Root Growth Plasticity and Nitrogen Metabolism Underpin Prolonged Cold Stress Tolerance at Tillering Stage in Japonica Rice. *Agronomy* **16**, 101 (2025).
57. Zhang, H., Sun, X. & Song, W. Physiological and growth characteristics of tomato seedlings in response to low root-zone temperature. *HortScience* **58**, 442–448 (2023).
58. Zhang, J. et al. Low soil temperature reducing the yield of drip irrigated rice in arid area by influencing anther development and pollination. *J. Arid Land.* **11**, 419–430 (2019).
59. Acuña, T. B. & Wade, L. J. Genotype× environment interactions for root depth of wheat. *F Crop Res.* **137**, 117–125 (2012).
60. MacMillan, K., Emrich, K., Piepho, H. P., Mullins, C. E. & Price, A. H. Assessing the importance of genotype× environment interaction for root traits in rice using a mapping population II: conventional QTL analysis. *Theor. Appl. Genet.* **113**, 953–964 (2006).
61. Mathew, I. & Shimelis, H. Genetic analyses of root traits: Implications for environmental adaptation and new variety development: A review. *Plant. Breed.* **141**, 695–718 (2022).
62. Pélabon, C., Hilde, C. H., Einum, S. & Gamelon, M. On the use of the coefficient of variation to quantify and compare trait variation. *Evol. Lett.* **4**, 180–188 (2020).
63. Zhou, L. et al. Genome-Wide Association Study of Brown Rice Weight Identifies an RNA-Binding Protein Antagonistically Regulating Grain Weight and Panicle Number. *Rice Sci.* **32**, 525–536 (2025).
64. Ganapati, R. K. et al. Genome-Wide Association Study and Haplotype Analysis Jointly Identify New Candidate Genes for Alkaline Tolerance at Seedling Stage in Rice. *Rice Sci.* **32**, 537–548 (2025).
65. Jo, S. et al. Analysis of quantitative trait loci and candidate gene exploration associated with cold tolerance in rice (Oryza sativa L.) during the seedling stage. *Front. Plant. Sci.* **15**, 1508333 (2025).
66. Yang, Y., Liu, J., Zhou, X., Liu, S. & Zhuang, Y. Identification of WRKY gene family and characterization of cold stress-responsive WRKY genes in eggplant. *PeerJ* **8**, e8777 (2020).
67. Song, J. et al. Genome-wide association mapping for cold tolerance in a core collection of rice (Oryza sativa L.) landraces by using high-density single nucleotide polymorphism markers from specific-locus amplified fragment sequencing. *Front. Plant. Sci.* **9**, 875 (2018).
68. Wang, D. et al. Genome-wide association mapping of cold tolerance genes at the seedling stage in rice. *Rice* **9**, 61 (2016).
69. Hund, A. et al. QTL controlling root and shoot traits of maize seedlings under cold stress. *Theor. Appl. Genet.* **109**, 618–629 (2004).
70. Liu, C. et al. Multi-trait genome-wide association studies reveal novel pleiotropic loci associated with yield and yield-related traits in rice. *J Integr. Agric* (2024).
71. Husaini, A. M. High-value pleiotropic genes for developing multiple stress-tolerant biofortified crops for 21st-century challenges. *Heredity (Edinb)*. **128**, 460–472 (2022).

72. Djanaguiraman, M., Prasad, P. V. V., Kumari, J. & Rengel, Z. Root length and root lipid composition contribute to drought tolerance of winter and spring wheat. *Plant. Soil.* **439**, 57–73 (2019).
73. Hund, A., Fracheboud, Y., Soldati, A. & Stamp, P. Cold tolerance of maize seedlings as determined by root morphology and photosynthetic traits. *Eur. J. Agron.* **28**, 178–185 (2008).
74. Bettembourg, M. et al. Genome-wide association mapping for root cone angle in rice. *Rice* **10**, 45 (2017).
75. To, H. T. M. et al. Unraveling the genetic elements involved in shoot and root growth regulation by jasmonate in rice using a genome-wide association study. *Rice* **12**, 69 (2019).
76. Xue, Z. et al. Unveiling Genetic Loci for Root Morphology and Salt Response at Rice Seedling Stage via Genome-Wide Association Studies. *Life* **15**, 1595 (2025).
77. Lv, Y. et al. New insights into the genetic basis of natural chilling and cold shock tolerance in rice by genome-wide association analysis. *Plant. Cell. Environ.* **39**, 556–570 (2016).
78. Yang, J. et al. Genome-wide association study reveals novel genetic loci contributing to cold tolerance at the germination stage in indica rice. *Plant. Sci.* **301**, 110669 (2020).
79. Li, C., Chen, B., Bu, F., Li, L. & Yu, Q. OsMYB305 on qATS1 positively regulates alkalinity tolerance at the seedling stage in japonica rice. *Plant. Growth Regul.* **103**, 733–745 (2024).
80. Wang, D. et al. Overexpression of OsMYB305 in rice enhances the nitrogen uptake under low-nitrogen condition. *Front. Plant. Sci.* **11**, 369 (2020).
81. Lan, Y. et al. Genome-wide characterization of the cytochrome P450 gene family in Solanum melongena and functional analysis of SmCYP82C1 under cold stress. *BMC Plant. Biol.* **25**, 1018 (2025).
82. Zheng, T. et al. Cyt02 encodes cytochrome P450 monooxygenase, increasing rice (Oryza sativa L.) resistance to sheath blight. *Crop J.* **13**, 92–103 (2025).
83. Liu, B., Song, Z. & Qi, X. Plant cytochrome P450 enzymes for bioactive metabolites biosynthesis, growth regulation, and stress adaptation. *Plant. Physiol.* **199**, kiaf297 (2025).
84. Lv, X. et al. Rice cytochrome P450 protein CYP71P1 is required for heat stress tolerance by regulating serotonin biosynthesis and ROS homeostasis. *Plants* **14**, 172 (2025).
85. Wang, A. et al. Rice (Oryza sativa L.) cytochrome P450 protein 716A subfamily CYP716A16 regulates disease resistance. *BMC Genom.* **23**, 343 (2022).
86. Nishiuchi, S., Watanabe, K., Sato, S., Takahashi, H. & Nakazono, M. Expression analysis of genes for cytochrome P450 CYP86 and glycerol-3-phosphate acyltransferase related to suberin biosynthesis in rice roots under stagnant deoxygenated conditions. *Plant Root* **15** (2015).
87. Tamiru, M. et al. A cytochrome P450, OsDSS1, is involved in growth and drought stress responses in rice (Oryza sativa L). *Plant. Mol. Biol.* **88**, 85–89 (2015).
88. Cai, L. et al. Nuclear encoded elongation factor EF-Tu is required for chloroplast development in rice grown under low-temperature conditions. *J. Genet. genomics = Yi chuan xue bao*. **49**, 502–505 (2022).
89. Ristic, Z., Bukovnik, U., Momčilović, I., Fu, J. & Prasad, P. V. Heat-induced accumulation of chloroplast protein synthesis elongation factor, EF-Tu, in winter wheat. *J. Plant. Physiol.* **165**, 192–202 (2008).
90. Bhadula, S. K. et al. Heat-stress induced synthesis of chloroplast protein synthesis elongation factor (EF-Tu) in a heat-tolerant maize line. *Planta* **212**, 359–366 (2001).
91. Wang, Y. et al. Overexpression of OsNAR2. 1 by OsNAR2. 1 promoter increases drought resistance by increasing the expression of OsPLDα1 in rice. *BMC Plant. Biol.* **24**, 321 (2024).

92. Yan, M. et al. Rice OsNAR2. 1 interacts with OsNRT2. 1, OsNRT2. 2 and OsNRT2. 3a nitrate transporters to provide uptake over high and low concentration ranges. *Plant. Cell. Environ.* **34**, 1360–1372 (2011).
93. Chen, J. et al. OsNAR2. 1 positively regulates drought tolerance and grain yield under drought stress conditions in rice. *Front. Plant. Sci.* **10**, 197 (2019).
94. Song, M. et al. OsNAR2. 1 interaction with OsNIT1 and OsNIT2 functions in root-growth responses to nitrate and ammonium. *Plant. Physiol.* **183**, 289–303 (2020).
95. Wu, J. et al. Nuclear translocation of OsMADS25 facilitated by OsNAR2. 1 in reponse to nitrate signals promotes rice root growth by targeting OsMADS27 and OsARF7. *Plant Commun* **4**, (2023).
96. Wu, J. et al. Nuclear Accumulation of OsMADS27 Was Promoted by OsNAR2. 1 in Response to Nitrate to Control Root Growth by Directly Targeting OsMADS57 in Rice. *Physiol. Plant.* **177**, e70553 (2025).
97. Kim, H. et al. Overexpression of PYL5 in rice enhances drought tolerance, inhibits growth, and modulates gene expression. *J. Exp. Bot.* **65**, 453–464 (2014).
98. Kim, H. et al. A rice orthologue of the ABA receptor, OsPYL/RCAR5, is a positive regulator of the ABA signal transduction pathway in seed germination and early seedling growth. *J. Exp. Bot.* **63**, 1013–1014 (2012).
99. Xu, R. et al. The OsWRKY7–OsVQ3 module regulates seedling-stage cold tolerance in rice. *Plant. J.* **124**, e70605 (2025).
100. Xia, C., Gong, Y., Chong, K. & Xu, Y. Phosphatase OsPP2C27 directly dephosphorylates OsMAPK3 and OsbHLH002 to negatively regulate cold tolerance in rice. *Plant. Cell. Environ.* **44**, 491–505 (2021).
101. Yi, J. et al. The rice gene DEFECTIVE TAPETUM AND MEIOCYTES 1 (DTM1) is required for early tapetum development and meiosis. *Plant. J.* **70**, 256–270 (2012).
102. Yu, S., Li, S., Wang, W. & Tang, D. OsCAMTA3 negatively regulates disease resistance to Magnaporthe oryzae by associating with OsCAMTAPL in rice. *Int. J. Mol. Sci.* **25**, 5049 (2024).
103. Kappara, S., Neelamraju, S. & Ramanan, R. Down regulation of a heavy metal transporter gene influences several domestication traits and grain Fe-Zn content in rice. *Plant. Sci.* **276**, 208–219 (2018).
104. Liu, J., Jie, W., Shi, X. A., Ding, Y. & Ding, C. Transcription elongation factors OsSPT4 and OsSPT5 are essential for rice growth and development and act with APO2. *Plant. Cell. Rep.* **42**, 1217–1231 (2023).
105. Ye, N. et al. Abscisic acid enhances trehalose content via OsTPP3 to improve salt tolerance in rice seedlings. *Plants* **12**, 2665 (2023).
106. Jiang, D., Chen, W., Gao, J., Yang, F. & Zhuang, C. Overexpression of the trehalose-6-phosphate phosphatase OsTPP3 increases drought tolerance in rice. *Plant. Biotechnol. Rep.* **13**, 285–292 (2019).
107. Qin, Z. et al. ABA biosynthesis rather than ABA catabolism is induced by low temperature and inhibits seed germination by activating OsTPP3. *Crop J.* **13**, 752–763 (2025).
108. Wang, Y. et al. The plasma membrane-localized OsNIP1; 2 mediates internal aluminum detoxification in rice. *Front. Plant. Sci.* **13**, 970270 (2022).
109. Morii, M. et al. The dual function of OsSWEET3a as a gibberellin and glucose transporter is important for young shoot development in rice. *Plant. Cell. Physiol.* **61**, 1935–1945 (2020).
110. Abbas, W. et al. The GW5-WRKY53-SGW5 module regulates grain size variation in rice. *New. Phytol*. **242**, 2011–2025 (2024).
111. Jiao, X. et al. Promotion of BR biosynthesis by miR444 is required for ammonium-triggered inhibition of root growth. *Plant. Physiol.* **182**, 1454–1466 (2020).

112. Hong, Z. et al. Loss-of-function of a rice brassinosteroid biosynthetic enzyme, C-6 oxidase, prevents the organized arrangement and polar elongation of cells in the leaves and stem. *Plant. J.* **32**, 495–508 (2002).
113. Huang, Y. H. et al. A translational regulator MHZ9 modulates ethylene signaling in rice. *Nat. Commun.* **14**, 4674 (2023).
114. Zhao, H. et al. The GDSL lipase MHZ11 modulates ethylene signaling in rice roots. *Plant. Cell.* **32**, 1626–1643 (2020).
115. Huang, J. et al. OsSNDP1, a Sec14-nodulin domain-containing protein, plays a critical role in root hair elongation in rice. *Plant. Mol. Biol.* **82**, 39–50 (2013).
116. Sommer, M. L., Zhou, Y. & Hochholdinger, F. Differential cold stress intensities drive unique morphological and transcriptomic changes in Zea mays root hairs. *BMC Genom.* **26**, 805 (2025).
117. Shen, W. et al. Auxin/ROS-Mediated Coordination of Lateral Root and Root Hair Development in Wheat (Triticum aestivum L.) Under Low-Temperature Stress. *Physiol. Plant.* **177**, e70563 (2025).

Figures

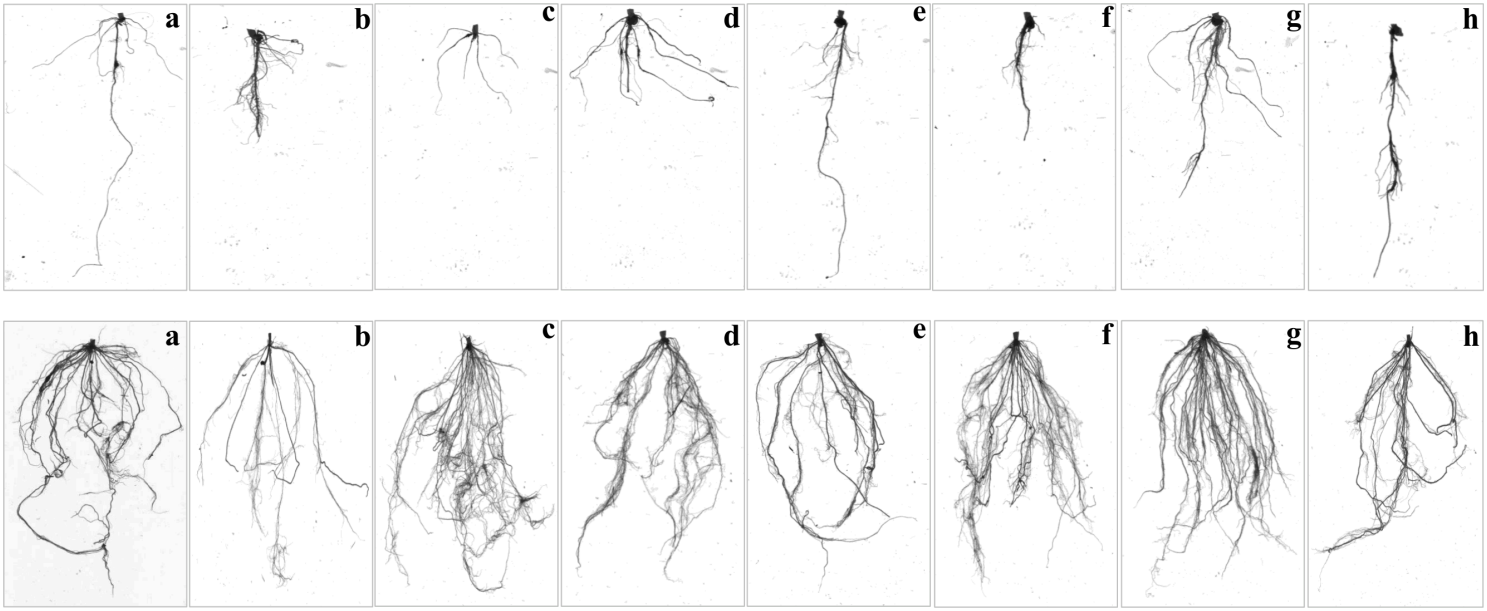


Figure 1

Phenotypic view of roots under cold and controlled conditions: Top (growth chamber cold condition as E1) and Bottom (greenhouse controlled condition as E2). Top and bottom images (a-h) are the same germplasm accessions (like a-a).

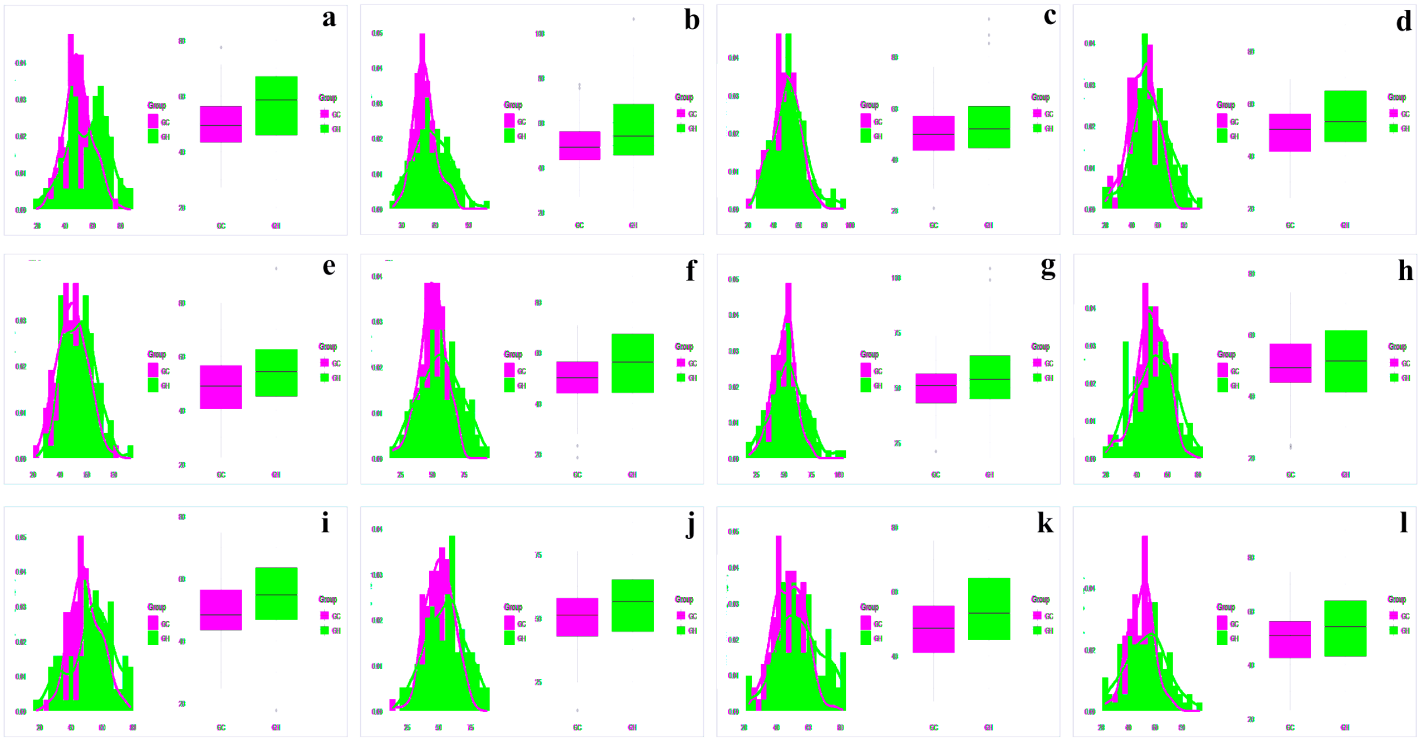


Figure 2

Frequency distribution of variation for 12 traits in 204 rice accessions: ARD=average root diameter (a); RC=root crossings (b); RF=root forks (c); RPA=root projected area (d); RV=root volume (e); TRL=total root length (f); TRSA=total root surface area (g); RT=root tips (h); FSW= fresh shoot weight (i); DSW= dry shoot weight (j); RFW= root fresh weight (k); RDW= root dry weight (l); across both environments, E1= Growth chamber cold condition and E2 = Greenhouse controlled condition.

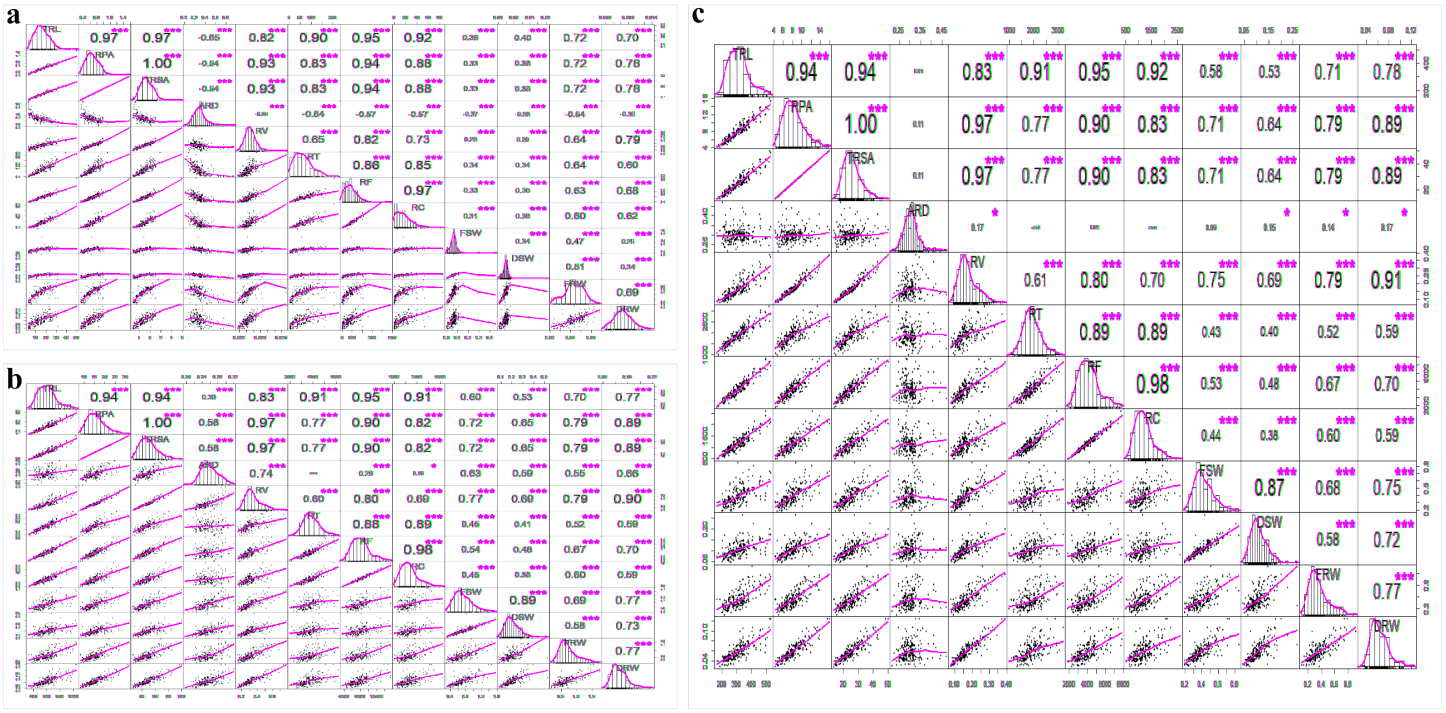


Figure 3

Pearson's correlation coefficients describing association of various root related traits in rice under two environmental conditions: Growth chamber cold condition (a), Greenhouse controlled condition (b), and Combined of both environments.

Supplementary Files

This is a list of supplementary files associated with this preprint. Click to download.

- TableS2.xlsx
- Fig.S6.tiff
- Fig.S5.tiff
- Fig.S4.tiff
- Fig.S3.tiff
- Fig.S1.tiff